J Solution Chem (2007) 36: 803–813
DOI 10.1007/s10953-007-9146-1

ORIGINAL PAPER

Li^+ Transport Mechanism in Oligo(Ethylene Oxide)s Compared to Carbonates

Oleg Borodin · G.D. Smith

Received: 17 August 2006 / Accepted: 24 December 2006 /
Published online: 27 April 2007

Abstract Molecular dynamics simulations have been performed on oligo(ethylene oxide)s of various molecular weights doped with the lithium bis(trifluoromethanesulfonyl)imide salt (LiTFSI) in order to explore the mechanism of Li^+ transport in materials covering the range from liquid electrolytes to prototypes for high molecular weight poly(ethylene oxide)-based polymer electrolytes. Good agreement between MD simulations and experiments is observed for the conductivity of electrolytes as a function of molecular weight. Unlike Li^+ transport in liquid ethylene carbonate (EC) that comes from approximately equal contributions of vehicular Li^+ motion (motion together with solvent) and Li^+ diffusion by solvent exchange, Li^+ transport in oligoethers was found to occur predominantly by vehicular motion. The slow solvent exchange of Li^+ in oligo(ethylene oxide)s highlights why high molecular weight amorphous polymer electrolytes with oligo(ethylene oxide)s solvating groups suffer from poor Li^+ transport. Ion complexation and correlation of cation and anion motion is examined for oligoethers and compared with that in EC.

Keywords Molecular dynamics simulations · Electrolytes · Lithium battery

1 Introduction

The desire to utilize lithium batteries for hybrid and electric vehicles has instigated a search for novel electrolytes with improved transport and electrochemical properties that would improve upon performance, cost and safety characteristics of traditional liquid electrolytes based upon mixtures of carbonates with a relatively high dielectric constant such as ethylene carbonate (EC) or propylene carbonate (PC) with carbonates or oligoethers that have lower dielectric constants such as 1,2-dimethoxyethane (DME) or dimethyl carbonate. Lithium batteries with solid polymer electrolytes (SPE) or plasticized polymer electrolytes have been widely explored as an alternative technology [1]. SPEs are formed by dissolving lithium

O. Borodin (✉) · G.D. Smith
Department of Materials Science & Engineering, University of Utah, 122 S. Central Campus Dr,
Rm 304, Salt Lake City, UT 84112-0560, USA
e-mail: borodin@eng.utah.edu

salts in a polymer matrix with linear, block-copolymer, or comb-branch architectures with oligo(ethylene oxide) being the most popular choice for solvating groups [1]. The SPEs combine ease of fabrication with good electrochemical stability, low flammability and toxicity, and might eliminate a need for a separator. Despite many advantages of SPEs over liquid electrolytes they exhibit low ambient temperature conductivity and low transference numbers preventing them from being used in batteries at high discharge rates for electronics and automotive applications [1].

We have initiated a series of molecular dynamics (MD) simulation studies aimed at obtaining a fundamental understanding of Li^+ transport in liquid and polymeric electrolytes. In this effort we have developed a quantum chemistry-based many-body polarizable force field [2–5] for oligoethers and carbonates doped with lithium bis(trifluoromethanesulfonyl)-imide (LiTFSI, $TFSI^- = CF_3SO_2NSO_2CF_3$) and other salts. The $TFSI^-$ anion was chosen because LiTFSI salts largely dissociate in poly(ethylene oxide) (PEO) matrices resulting in cation and anion motion being uncorrelated [6]. The developed force field [3, 7] accurately predicts the Li^+ cation environment, ion and solvent diffusion coefficients, electrolyte conductivity and the degree of ion aggregation in PEO SPEs and carbonate-based liquid electrolytes and ionic liquids [8, 9] over a wide range of temperatures and salt concentrations.

The earlier reports [3, 10–27] focused on understanding the Li^+ environment, its transport mechanisms in PEO-based/Li salts SPEs and in EC as it is the most widely used component of liquid electrolytes and is used as a plasticizer in gel electrolytes. In this contribution we focus on exploring the mechanisms of Li^+ transport in various oligo(ethylene oxide)s ranging from 1,2-dimethoxyethane (DME, $H-(CH_2OCH_2)_n-H$, EO_2 with $n = 2$) to pentaglyme (EO_n, $n = 6$) to unentangled PEO ($n = 54$) doped with LiTFSI and compare our finding with the results with the previous finding in EC/LiTFSI [26] and PEO/LiTFSI [3]. Previous MD simulations [28–33] of lithium salts in aprotic liquids provided some insight into Li^+ coordination but there is no investigation of the mechanism of Li^+ transport through an electrolyte, dynamic correlation of ion motion or even calculated electrolyte conductivity with the exception of one study [32].

2 Simulation Methodology

The MD simulation methodology and methodology for extracting ion conductivity and self-diffusion coefficients were previously described [3, 26]. Briefly, a Noe-Hoover thermostat and a barostat were used to control the temperature and pressure with the associated frequencies 10^{-2} fs^{-1} and 10^{-3} fs^{-1} [34]. Bond lengths were constrained using the Shake algorithm [34]. The Ewald summation method [34] was used for treatment of long-range electrostatic forces between partial charges, and between partial charges and induced dipoles for the many-body polarizable potential. The Ewald convergence parameter, α, was set to 8 Å. The number of reciprocal space vectors was set to 6^3. A tapering function was used for scaling the induced dipole-induced dipole interactions to zero at the cutoff of 10 Å with scaling starting at 9 Å. A multiple time-step reversible reference system propagator algorithm [35] was employed, with a timestep of 0.5 fs for bonding, bending and torsional motions, a 1.5 fs timestep for non-bonded interactions within a 6.5 Å sphere and a 3.0 fs timestep for non-bonded interactions between 6.5 and 10.0 Å, and the reciprocal space part of the Ewald summation. Coordinates were stored every 1 ps.

A previously developed force field was used [4]. The equilibration and production run length for PEO($= EO_{54}$)/LiTFSI, pentaglyme($= EO_6$)/LiTFSI, DME($= EO_2$)/LiTFSI and EC/LiTFSI electrolytes are summarized in Table 1. All electrolytes were simulated using

Table 1 Length of MD simulations, fractions of free ions α_s (with $r(\mathrm{Li}^+\text{-}\mathrm{N}^{\mathrm{TFSI}^-}) > 5$ Å), degree of ion uncorrelated motion (α_d)

Salt concentration (EO : Li or EC : Li)	Temperature (K)	Equilibration run length (ns)	Production run length (ns)	α_s	α_d
EC/LiTFSI					
10	393	0.5	3	0.29	0.55
10	363	1	7	0.34	0.63
10	333	3	28	0.31	0.63
10	313	2	29	0.32	0.66
DME/LiTFSI					
20	393	1	1	0.19	0.30
20	363	1	8	0.28	0.42
20	333	1	3	0.38	0.50
20	308	3	14.2	0.35	0.48
DME/LiTFSI with dissociated salt[a]					
20	363	0.5	5	1	0.7
DME/LiTFSI with increased Li^+-DME residence time					
20	363	0.2	1	1	0.7
EO_6/LiTFSI					
20	393	3	4	0.8	0.75
20	363	3	26	0.92	0.70
20	333	4	9	0.9	0.65
10	393	3	32	0.74	0.75
10	363	3	5	0.85	0.6
PEO(= EO_{54})/LiTFSI					
39	423	5	20	0.91	0.85
39	393	3	16	0.97	0.91
20	423	5	29	0.88	0.92
20	393	3	52	0.95	0.92
20	363	7	40	0.94	0.82
20	333	3	10	0.93	0.90
10	423	3	18	0.70	0.78
10	393	5	10.5	0.70	0.77

[a]Repulsion parameters for $\mathrm{Li}^+\text{-}\mathrm{O}^{\mathrm{TFSI}^-}$ interactions were changed to $A = 99530.0$ kcal·mol^{-1}, $B = 4.0$ Å^{-1} in $U^{\mathrm{rep}}(r) = A\exp(-Br_{ij})$

periodic boundary conditions with simulation cells of linear dimensions from 2.8 to 3.6 nm. Ewald summation was used to treat interactions between permanent charges with permanent charges and induced dipoles. A reaction field was used for treatment of induced dipole–induced dipole interactions with $\varepsilon = 90$ for simulations of EC liquid at 313 K only.

3 Structural Properties

The cumulative number of ether oxygen (EO) and $TFSI^-$ oxygen atoms tightly complexing a Li^+ cation ($r_{Li^+\text{-EO}} < 2.8$ Å) was approximately 4.5 for all oligoether-based electrolytes. The Li^+ environment in pentaglyme was similar to that previously reported [3] for PEO/LiTFSI with approximately 50% of the Li^+ cations being complexed by one pentaglyme molecule and the remaining cations being complexed by two pentaglyme chains. For EO : Li = 20, salt concentration at 363 K, the fraction of free ions that are uncomplexed by counterions ($r(Li^+\text{-}N^{TFSI^-}) > 5$ Å), denoted as α_s, is reported in Table 1. Increasing molecular weight and decreasing temperature yields a larger fraction of free ions. Interestingly, the temperature dependence of free ions in DME is noticeably stronger than that for EC/LiTFSI.

4 Transport Mechanism

Ion and solvent self-diffusion coefficients from MD simulations and experimental data are shown in Fig. 1 as a function of the solvent molecular weight for a EO:Li = 20, salt concentration at 333 K. Good agreement between simulation predictions and pgf-NMR measurements [6] is seen in Fig. 1. This agreement highlights the ability of MD simulations with our quantum-chemistry based force field to accurately predict ion and solvent transport in oligo(ethylene oxide)/LiTFSI electrolytes. Similar agreement with experiments was observed for other temperatures and salt concentrations [3, 7, 23]. As the solvent molecular weight increases, Li^+ diffusion gradually becoming faster than solvent diffusion indicating that exchange of solvating groups (sites) becomes increasingly important for Li^+ cation motion with increasing molecular weight of the oligo(ethylene oxide).

Our primary goal is to understand what fraction of Li^+ transport in liquid electrolytes comes from vehicular motion, i.e., motion of the cation together with its first solvation shell and what fraction comes from exchange of solvent molecules and how these contributions to Li^+ transport depend upon the molecular weight of the oligo(ethylene oxide). We quantify contributions of vehicular and solvent-exchange contributions to Li^+ diffusion by first considering the residence time of a solvent molecule in the Li^+ first coordination shell, then calculate the distance a Li^+ travels with the solvent (i.e., the distance traveled by the Li^+ cation on the solvent residence time scale) relative to the size of a solvent molecule. The longer the Li^+ travels with the solvent molecule the larger the contribution of the vehicular mechanism to the total Li^+ transport. Understanding the solvent residence times near Li^+ is also important for prediction of electrolyte viscosity from molecular based models of ion salvation [36].

The residence time autocorrelation function (ACF) for the solvent to be present in the Li^+ first solvation shell ($r_{Li^+\text{-EO}} < 2.8$ Å) was determined as follows

$$P_{\text{solvent-Li}^+}(t) = \frac{\langle H_{ij}(t) H_{ij}(0) \rangle}{\langle H_{ij}(0) H_{ij}(0) \rangle}, \tag{1}$$

where $H_{ij}(t)$ is 1 if Li^+ cations i have at least two EO from the same solvent molecule j in its first solvation shell and zero otherwise, $\langle\ \rangle$ denotes the average over all time origins and pairs of Li^+–solvent molecules. The mean residence time, τ_{res}, was calculated from $\exp(-t/\tau_{res})$ fits to the $P_{\text{solvent-Li}^+}(t)$ distribution functions. They are summarized in Fig. 2 together with results from previous simulations [26] of EC/LiTFSI. The solvent mean residence time increases in the order EC < DME < EO_6 < PEO and exhibits approximately the

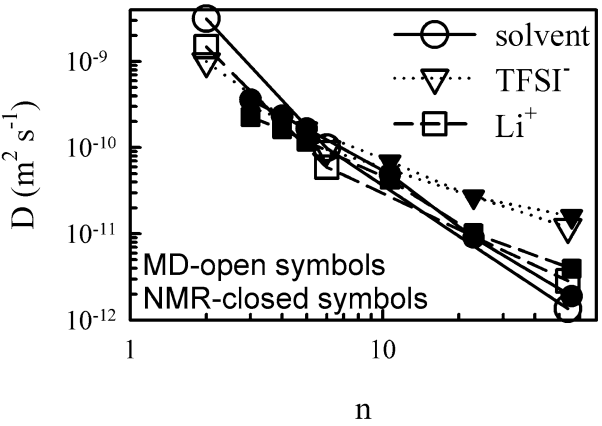

Fig. 1 Ion and solvent diffusion in $H-(CH_2OCH_2)_n-H$/LiTFSI electrolytes, EO : Li = 20 at 393 K from MD simulations and pgf-NMR experiments [6]

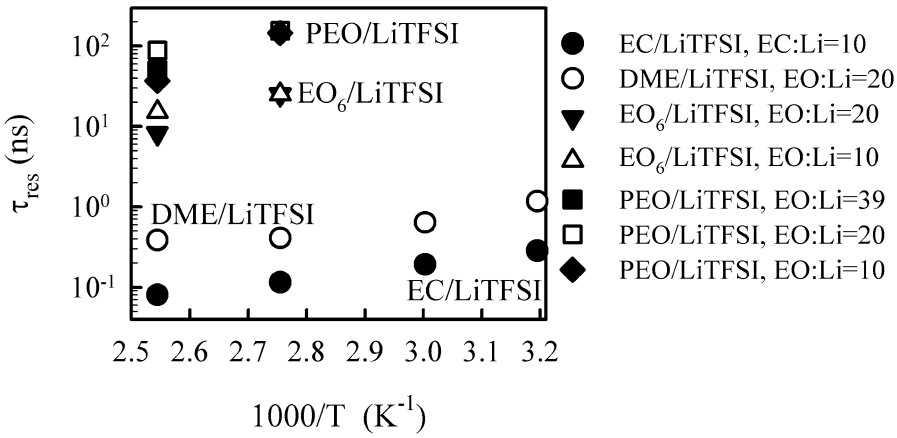

Fig. 2 The Li^+-solvent residence time ($\tau_{res.}$)

same near-Arrhenius temperature dependence as the ion and solvent self-diffusion coefficients [3, 26]. Lower EC residence time near Li^+ compared to the DME residence time near Li^+ is somewhat unexpected, because EC has a higher viscosity and lower self-diffusion coefficient compared to DME and yields similar fractions of free ions (α_s in Table 1). The mean solvent residence time increases dramatically (almost two orders of magnitude) when the oligo(ethylene oxide) molecular weight is increased from DME to pentaglyme and a factor of 3–10 with further increase of the PEO degree of polymerization to $n = 54$. This dependence of the solvent residence time on molecular weight is greater than that observed for the Li^+ diffusion coefficient or for the rate of conformational dynamics for the polymer (a decrease of about a factor of three). The greater complexation energy of Li^+ and pentaglyme compared to Li^+ complexation with DME and higher pentaglyme viscosity accounts for the large difference in the mean solvent residence times.

The average distance a Li^+ cation travels while residing (complexed to a given solvent molecule) [37], denoted by $L_{res.}$, is equal to the square root of the Li^+ mean-square displacement during an average time between solvent exchanges, $\tau_{residence}$, as indicated in Fig. 3a.

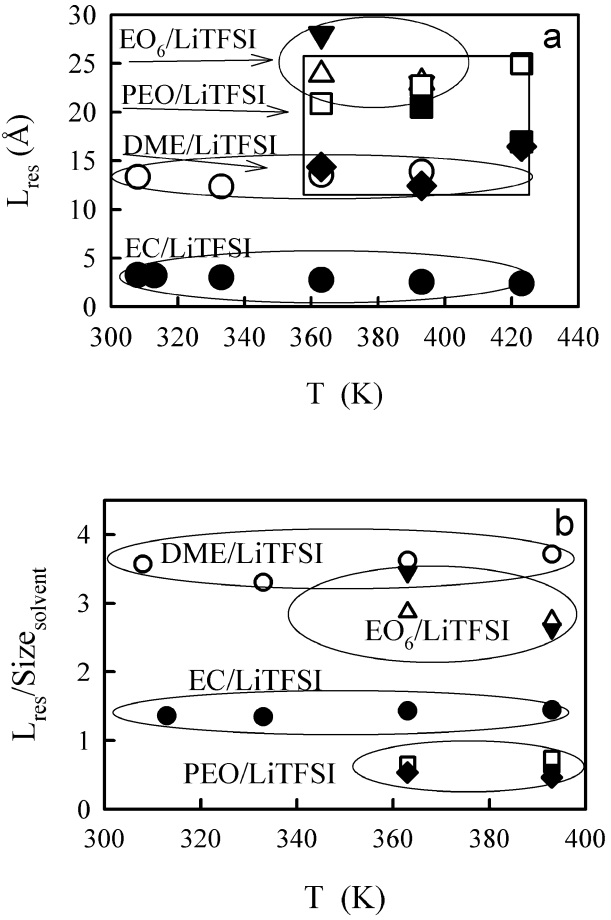

Fig. 3 **a** The MSD of Li^+ during one Li^+-chain residence time; **b** the same divided by the solvent molecular size ($S_{solv.}$). Symbols are the same as in Fig. 2

A Li^+ cation moves with EC approximately 4 Å with DME around 14 Å and with pentaglyme about 20–30 Å, and 12–25 Å with PEO.

In order to quantify the contribution of vehicular motion to Li^+ cation transport in liquid electrolytes (EC, DME, EO_6) we have normalized the mean distance that the Li^+ cation travels with a solvent molecule by the size of the solvent molecule, as shown in Fig. 3b, where the molecular size, $S_{solv.}$, was calculated as twice the radius of gyration. Hence here we show $L_{res.}/S_{solv.}$, the number of solvent molecular diameters a Li^+ cation moves with a solvent molecule before it exchanges solvent. The more solvent molecule diameters traveled before solvent exchange, the greater the contribution of the vehicular mechanism to the total Li^+ cation transport for liquid electrolytes. This supposition will be verified later through simulations, in which a Li^+ is forced to move together with the solvent. We observe from Fig. 3b that a Li^+ exchanges EC after traveling only 1.4 solvent sizes (molecular diameters). We estimate contributions to the mean-square displacement of a Li^+ cation after $\tau_{residence}$ using the

$$L_{res.}^2 = MSD_{vehicular} + MSD_{structure} = MSD_{vehicular} + S_{solv.}^2. \quad (2)$$

Dividing by $S^2_{\text{solv.}}$ yields

$$(L_{\text{res.}}/S_{\text{solv.}})^2 = MSD_{\text{vehicular}}/S^2_{\text{solv.}} + 1 \tag{3}$$

rearranging yields

$$MSD_{\text{vehicular}}/S^2_{\text{solv.}} = \frac{\text{vehicular}}{\text{solvent exchange}} = (L_{\text{res.}}/S_{\text{solv.}})^2 - 1. \tag{4}$$

The assumption is made here that the *MSD* (mean-square displacement) of the Li^+ cation due to exchange of solvent is given by the size of the solvent, $S_{\text{solv.}}$, molecule. Applying Eq. 4 to EC/LiTFSI yields a ratio $\frac{\text{vehicular}}{\text{solvent exchange}} = 1$, thus indicating similar contributions from vehicular and solvent exchange to the total Li^+ transport. This agrees with our previous observation [26] that the vehicular mechanism accounts for about 50% of the Li^+ transport in EC/LiTFSI that was made by forcing Li^+ to move with its first coordination shell and the observation of a drop in the self-diffusion coefficient by a factor of two. In DME/LiTFSI a Li^+ cation moves 3.3–3.7 solvent diameters before exchanging solvent. Here application of Eq. 4 yields $\frac{\text{vehicular}}{\text{solvent exchange}} = (12 \pm 2)$, indicating a dominance of the vehicular mechanism for Li^+ cation transport in DME. In order to confirm the above conclusion for DME/LiTFSI, we performed two additional simulations of this electrolyte at 363 K, EO:Li = 20. In the first simulation we artificially dissociated the LiTFSI salt by increasing repulsion between Li^+ and O^{TFSI^-} in order to measure Li^+ transport in DME with completely dissociated $Li^+/TFSI^-$. In the second simulation Li^+ was forced to move together with DME from its first solvation shell by additional interactions included for the Li^+ and EO shown in Eq. 5,

$$U^{\text{add}}(r) = -A \exp[-B(r - r_0)^2] \tag{5}$$

where r is the distance between Li^+ and EO, $A = 50$ kcal·mol^{-1}, $B = 50$ Å^{-1} and $r_0 = 1.985$ Å. The parameters of the $U^{\text{add}}(r)$ functions are chosen in such a way to keep the structure of the Li^+ coordination shell as close as possible to that for the DME/LiTFSI in the dissociated electrolyte as shown in Fig. 4, while significantly (by a factor of 4) increasing the DME residence time near Li^+. Note that ions in the second simulation will also be dissociated because of the increased Li^+/DME interactions. We found that the ion and solvent

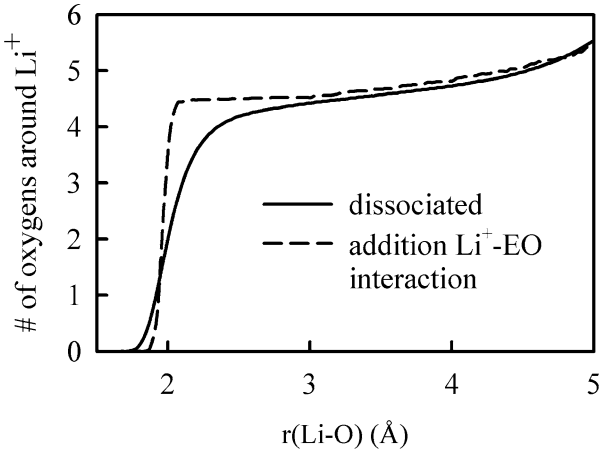

Fig. 4 Running coordination number of ether oxygen atoms around a Li^+ cation for DME/LiTFSI, EO : Li = 20 at 363 K for dissociated salt electrolyte (increased Li^+/O^{TFSI^-} repulsion) and for the one with increased Li^+/EO interactions (see Eq. 5)

diffusion coefficients of the DME/LiTFSI with the dissociated salt and that with an additional $U^{\text{add}}(r)$ interaction between Li^+ and O^{TFSI^-} are within 10% of each other validating our analysis based upon Eq. 4 that allowed us to conclude that the solvent exchange-based diffusion contribution to the Li^+ motion in DME is small (<10%). For the EO_6/LiTFSI electrolyte we obtain $\frac{\text{vehicular}}{\text{solvent exchange}} = (8 \pm 2.5)$, also indicating dominance of the vehicular diffusion mechanism for Li^+ transport in EO_6 consistent with our previous observations for the EO_{12}/LiTFSI electrolyte [23].

The $L_{\text{res.}}/S_{\text{solv.}}$ ratio of (0.6 ± 0.15) for PEO(= EO_{54})/LiTFSI shown in Fig. 3b indicates that for this molecular weight Li^+ moves less than one size of a PEO chain before its jumps to another chain, clearly demonstrating that the mechanism of Li^+ motion is no longer dominated by the vehicular transport as was the case for DME/LiTFSI and EO_6/LiTFSI. In fact, Li^+ diffusion in polymer electrolytes is a result of three types of Li^+ motion: (a) moving along the polymer backbone, (b) moving with the polymer segments, and (c) interchain (or intersegment) transfer between chains as was discussed previously in detail [3]. Both motion with a polymer segment and along the segment are subdiffusive with mean-square displacements, *MSD*, $MSD \sim t^{0.6}$ and $MSD \sim t^{0.5}$, respectively, where t is time. The interchain transfers are needed to achieve Li^+ diffusive behavior $MSD \sim t$. The L_{res} in Fig. 3a is the combined distance a Li^+ travels with the polymer segment and along PEO chains in between interchain transfers. Note, that Eq. 4 cannot be straightforwardly applied to polymer electrolytes because the solvent exchange contribution to Li^+ diffusion in polymeric materials is given by a combination of interchain Li^+ transfer and Li^+ moving along polymer chains.

5 Influence of DME Conformational Dynamics on Li^+ Transport

A previous study of PEO/LiTFSI demonstrated that torsional relaxation is coupled with the dynamics of Li^+ and $TFSI^-$ ions [3]. Here, we wish to understand the influence of conformational dynamics on Li^+ transport in DME. We have increased the DME conformational barriers by 1 kcal·mol^{-1} for DME/LiTFSI, EO:Li = 20 at 363 K and simulated for 1 ns. An increase of the conformational barriers slowed down torsional relaxation of the O−C−C−O torsion by a factor of three as measured by the decay of the torsional autocorrelation functions [3]. The resulting electrolyte has essentially the same DME exchange rate as the electrolyte simulated with the original force field. The ion and solvent diffusion coefficients for the electrolytes with decreased conformational flexibility yielded solvent and ion self-diffusion coefficients within 15% of those of the original force field indicating that Li^+ transport in a liquid DME electrolyte is largely insensitive to the DME conformational dynamics.

6 Ion Correlations

MD simulations allow one to study the relation between Li^+ and $TFSI^-$ aggregation (structural property) and the correlation of ion motion (dynamic property) in the same set of simulations. Moreover, simulations of electrolytes with the LiTFSI salt, which is completely dissociated by increasing repulsion between Li^+ and $TFSI^-$, present a unique opportunity to study the extent of correlation of the Li^+ and $TFSI^-$ motion separated by solvent. The dynamic degree of uncorrelated ion motion, α_d, was calculated using Eqs. 6–8. The ionic

conductivity, λ, is given [10]

$$\lambda = \lim_{t\to\infty} \frac{e^2}{6tVk_BT} \sum_{i,j}^{N} z_i z_j \langle([\mathbf{R}_i(t) - \mathbf{R}_i(0)])([\mathbf{R}_j(t) - \mathbf{R}_j(0)])\rangle \quad (6)$$

where e is the electron charge, V is the volume of the simulation box, k_B is Boltzmann's constant, T is the temperature, t is time, z_i and z_j are the charges over ions i and j in electrons, and $\mathbf{R}_i(t)$ is the displacement of the ion i during time t. The summation is performed over all ions, $\langle\ \rangle$ denote the ensemble average and N is the total number of ions in the simulation box, and $\lambda^{\text{app}}(t)$ is the apparent time-dependent conductivity. The degree of uncorrelated ion motion, α, is typically measured as the ratio of the collective (total) charge transport (given by λ) to the charge transport due to self-diffusion only (a limit of completely dissociated and uncorrelated motion) $\lambda_{\text{uncorr.}}$ and is given by

$$\lambda^{\text{app}}_{\text{uncorr.}}(t) = \frac{e^2}{Vk_BT}\left(n_{\text{Li}^+} D^{\text{app}}_{\text{Li}^+} + n_{\text{Li}^+} D^{\text{app}}_{\text{TFSI}^-}\right) = \frac{e^2}{6tVk_BT} \sum_{i}^{N} z_i^2 \langle[\mathbf{R}_i(t) - \mathbf{R}_i(0)]^2\rangle \quad (7)$$

$$\alpha_d = \frac{\lambda}{\lambda_{\text{uncorr.}}} = \lim_{t\to\infty} \alpha_d(t) = \lim_{t\to\infty} \frac{\lambda^{\text{app}}(t)}{\lambda^{\text{app}}_{\text{uncorr.}}(t)}. \quad (8)$$

Here n_i is the number of atoms of type i. Thus, $\alpha_d = 1$ corresponds to uncorrelated ion motion, while $\alpha_d = 0$ if all of the cations only move together with the anions. Table 1 summarizes $\alpha_d = 1$ for simulated electrolytes and compares it with the fraction of free ions obtained from structural analysis, α_s. We estimate the uncertainty of α_d as being around 0.1. The α_d values are consistent with those experimentally estimated from coordinated pgf-NMR and conductivity measurements [6, 38]. The cation and anion motions become less correlated in oligoether-based solvents with increasing solvent molecular weight in agreement with experimental observations [6]. This tendency correlates well with the increasing fraction of free ions, α_s, with increasing oligoether molecular weight or decreasing temperature. Table 1 shows that α_d is larger than α_s for EC/LiTFSI and DME/LiTFSI. The α_d is greater than α_s because of the motion of charged aggregates occurring in the simulations. Interestingly, for EO_6/LiTFSI and dilute PEO/LiTFSI we find $\alpha_d < \alpha_s$ indicating correlations between solvent separated ions are stronger than the contribution to charge transport due to charged aggregates.

Another question we would like to tackle is the degree of ion correlation between Li^+ and $TFSI^-$ separated by one ether solvent molecule. To understand this behavior we analyzed ion correlations in DME/LiTFSI dilute electrolyte EO:Li = 20 where complete salt dissociated was achieved by either increasing Li^+/DME interactions or increasing repulsion between Li^+ and $TFSI^-$. For such a dissociated dilute DME/LiTFSI electrolyte ($\alpha_s = 1$) we observe a noticeable dynamic correlation of ion motion, $\alpha_d = 0.7$. In contrast, $\alpha_d = 1$ was observed for the dissociated, $\alpha_s = 1$, EC/LiTFSI, EC:Li = 10 electrolyte at 363 K previously simulated by us [26], consistent with experimental observations of $\alpha_d > 0.93$ for the infinite dilution limit of Li-salts in carbonates [38]. The lower dielectric constant of DME (≈ 7.4 at 298 K from MD simulations and 7.18 from experiment [39]) apparently is responsible for the correlation of solvent-separated ions in DME, whereas the much larger dielectric constant of EC (≈ 71 at 313 K from MD and 90.5 from experiments [40]) weakens the Li^+/$TFSI^-$ interactions and results in uncorrelated Li^+ and $TFSI^-$ motion in EC/LiTFSI.

7 Conclusions

Our MD simulations studies have predicted the transport and structural properties of liquid electrolytes in good agreement with experiments. Analysis of the Li^+ transport mechanism indicates that the Li^+ transport in oligoethers (DME, pentaglyme) is dominated by the Li^+ vehicular motion together with its solvation shell, unlike the Li^+ transport mechanism in EC/LiTFSI, where Li^+ is transported by equal contributions from vehicular motion with the solvent and solvent exchange.

Acknowledgements The authors are grateful for the financial support of this work by the Assistant Secretary for Energy Efficiency and Renewable Energy, Office of FreedomCAR and Vehicle Technologies of the U.S. Department of Energy under Contract No. DE-AC02-05CH11231 on PO No. 6515401.

References

1. Tarascon, J.M., Armand, M.: Issues and challenges facing rechargeable lithium batteries. Nature **414**, 359–367 (2001)
2. Borodin, O., Smith, G.D.: Development of quantum chemistry-based force fields for poly(ethylene oxide) with many-body polarization interactions. J. Phys. Chem. B **107**, 6801–6812 (2003)
3. Borodin, O., Smith, G.D.: Mechanism of ion transport in amorphous poly(ethylene oxide)/LiTFSI from molecular dynamics simulations. Macromolecules **39**, 1620–1629 (2006)
4. Borodin, O., Smith, G.D.: Development of many-body polarizable force fields for Li-battery components: 1. Ether, alkane, and carbonate-based solvents. J. Phys. Chem. B **110**, 6279–6292 (2006)
5. Borodin, O., Smith, G.D., Douglas, R.: Force field development and MD simulations of poly(ethylene oxide)/$LiBF_4$ polymer electrolytes. J. Phys. Chem. B **107**, 6824–6837 (2003)
6. Hayamizu, K., Akiba, E., Bando, T., Aihara, Y.: H-1, Li-7, and F-19 nuclear magnetic resonance and ionic conductivity studies for liquid electrolytes composed of glymes and polyetheneglycol dimethyl ethers of $CH_3O(CH_2CH_2O)(n)CH_3$ (n = 3–50) doped with $LiN(SO_2CF_3)(2)$. J. Chem. Phys. **117**, 5929–5939 (2002)
7. Borodin, O., Smith, G.D.: Development of many-body polarizable force fields for Li-battery applications: 2. LiTFSI-doped oligoether, polyether, and carbonate-based electrolytes. J. Phys. Chem. B **110**, 6293–6299 (2006)
8. Borodin, O., Smith, G.D., Henderson, W.: Li^+ cation environment, transport and mechanical properties of the LiTFSI doped *N*-methyl-*N*-alkylpyrrolidinium $^+TFSI^-$ ionic liquids. J. Phys. Chem. B **110**, 16879–16886 (2006)
9. Borodin, O., Smith, G.D.: Structure and dynamics of (*N*-methyl-*N*-propylpyrrolidinium)$^+$(TFSI)$^-$ ionic liquid from molecular dynamics simulations. J. Phys. Chem. B **110**, 11481–11490 (2006)
10. Muller-Plathe, F., van Gunsteren, W.F.: Computer simulation of a polymer electrolyte: Lithium iodide in amorphous poly(ethylene oxide). J. Chem. Phys. **103**, 4745–4756 (1995)
11. Smith, G.D., Borodin, O., Pekny, M., Annis, B., Londono, D., Jaffe, R.L.: Polymer force fields from ab initio studies of small model molecules: Can we achieve chemical accuracy? Spectrochim. Acta A Mol. Biomol. Spectrosc. **53**, 1273–1283 (1997)
12. Borodin, O., Smith, G.D.: Molecular dynamics simulations of poly(ethylene oxide)/LiI melts 1. Structural and conformational properties. Macromolecules **31**, 8396–8406 (1998)
13. Borodin, O., Smith, G.D.: Molecular dynamics simulations of poly(ethylene oxide)/LiI melts 2. Dynamic properties. Macromolecules **33**, 2273–2283 (2000)
14. Sawa, F., Takimoto, J., Aoyagi, T., Fukunaga, H., Shoji, T., Doi, M.: Molecular dynamics study of poly(ethylene oxide) containing LiI salt. Progr. Theor. Phys. Suppl. 408–409 (2000)
15. Hyun, J.K., Dong, H.T., Rhodes, C.P., Frech, R., Wheeler, R.A.: Molecular dynamics simulations and spectroscopic studies of amorphous tetraglyme ($CH_3O(CH_2CH_2O)(4)CH_3$) and tetraglyme:$LiCF_3SO_3$ structures. J. Phys. Chem. B **105**, 3329–3337 (2001)
16. Triolo, A., Arrighi, V., Triolo, R., Passerini, S., Mastragostino, M., Lechner, R.E., Ferguson, R., Borodin, O., Smith, G.D.: Dynamic heterogeneity in polymer electrolytes. Comparison between QENS data and MD simulations. Phys. B **301**, 163–167 (2001)
17. van Zon, A., de Leeuw, S.W.: A Rouse model for polymer electrolytes. Electrochim. Acta **46**, 1539–1544 (2001)

18. Ferreira, B.A., Muller-Plathe, F., Bernardes, A.T., De Almeida, W.B.: A comparison of Li^+ transport in dimethoxyethane, poly(ethylene oxide) and poly(tetramethylene oxide) by molecular dynamics simulations. Solid State Ionics **147**, 361–366 (2002)
19. Kuppa, V., Manias, E.: Computer simulation of PEO/layered-silicate nanocomposites: 2. Lithium dynamics in PEO/Li^+ montmorillonite intercalates. Chem. Mater. **14**, 2171–2175 (2002)
20. Borodin, O., Smith, G.D., Bandyopadhyaya, R., Redfern, P., Curtiss, L.A.: Molecular dynamics study of nanocomposite polymer electrolyte based on poly(ethylene oxide)/LiBF4. Model Simul. Mater. Sci. Eng. **12**, S73–S89 (2004)
21. Siqueira, L.J.A., Ribeiro, M.C.C.: Molecular dynamics simulation of the polymer electrolyte poly(ethylene oxide)/$LiClO_4$. I. Structural properties. J. Chem. Phys. **122**, 194911/1-8 (2005)
22. Duan, Y.H., Halley, J.W., Curtiss, L., Redfern, P.: Mechanisms of lithium transport in amorphous polyethylene oxide. J. Chem. Phys. **122**, 054702/1-8 (2005)
23. Borodin, O., Smith, G.D., Geiculescu, O., Creager, S.E., Hallac, B., DesMarteau, D.: Li^+ transport in lithium sulfonylimide-oligo(ethylene oxide) ionic liquids and oligo(ethylene oxide) doped with LiTFSI. J. Phys. Chem. B **110**, 24266–24274 (2006)
24. Siqueira, L.J.A., Ribeiro, M.C.C.: Molecular dynamics simulation of the polymer electrolyte poly(ethylene oxide)/$LiClO_4$. II. Dynamical properties. J. Chem. Phys. **125**, 214903–214908 (2006)
25. Annis, B.K., Borodin, O., Smith, G.D., Grant, D., Benmore, C.J., Soper, A.K., Londono, J.D.: The structure of a poly(ethylene oxide) melt from neutron scattering and molecular dynamics simulations. J. Chem. Phys. **115**, 10998–11003 (2001)
26. Borodin, O., Smith, G.D.: LiTFSI Structure and transport in ethylene carbonate from molecular dynamics simulations. J. Phys. Chem. B **110**, 4971–4977 (2006)
27. Borodin, O., Smith, G.D.: Molecular dynamics simulations of comb-branched poly(epoxide ether)-based polymer electrolytes. Macromolecules **40**, 1252–1258 (2007)
28. Li, T., Balbuena, P.B.: Theoretical studies of lithium perchlorate in ethylene carbonate, propylene carbonate, and their mixtures. J. Electrochem. Soc. **146**, 3613–3622 (1999)
29. Balbuena, P.B., Lamas, E.J., Wang, Y.X.: Molecular modeling studies of polymer electrolytes for power sources. Electrochim. Acta **50**, 3788–3795 (2005)
30. Masia, M., Probst, M., Rey, R.: Ethylene carbonate-Li^+: A theoretical study of structural and vibrational properties in gas and liquid phases. J. Phys. Chem. B **108**, 2016–2027 (2004)
31. Tasaki, K.: Computational study of salt association in Li-ion battery electrolyte. J. Electrochem. Soc. **149**, A418–A425 (2002)
32. Newman, J., Thomas, K.E., Hafezi, H., Wheeler, D.R.: Modeling of lithium-ion batteries. J. Power Sources **119**, 838–843 (2003)
33. Soetens, J.C., Millot, C., Maigret, B.: Molecular dynamics simulation of $Li(+)BF_4(-)$ in ethylene carbonate, propylene carbonate, and dimethyl carbonate solvents. J. Phys. Chem. A **102**, 1055–1061 (1998)
34. Frenkel, D., Smit, B.: Understanding Molecular Simulation: From Algorithms to Applications, 2nd edn. Academic Press (2002)
35. Martyna, G.J., Tuckerman, M., Tobias, D.J., Klein, M.L.: Explicit reversible integration algorithms for extended systems. Mol. Phys. **87**, 1117–1157 (1996)
36. Gering, K.L.: Prediction of electrolyte viscosity for aqueous and non-aqueous systems: Results from a molecular model based on ion solvation and a chemical physics framework. Electrochim. Acta **51**, 3125–3138 (2006)
37. Smith, G.D., Borodin, O., Bedrov, D., Paul, W., Qiu, X., Ediger, M.D.: C-13 NMR spin-lattice relaxation and conformational dynamics in a 1,4-polybutadiene melt. Macromolecules **34**, 5192–5199 (2001)
38. Aihara, Y., Sugimoto, K., Price, W.S., Hayamizu, K.: Ionic conduction and self-diffusion near infinitesimal concentration in lithium salt-organic solvent electrolytes. J. Chem. Phys. **113**, 1981–1991 (2000)
39. Cote, J.F., Brouillette, D., Desnoyers, J.E., Rouleau, J.F., St-Arnaud, J.M., Perron, G.: Dielectric constants of acetonitrile, gamma-butyrolactone, propylene carbonate, and 1,2-dimethoxyethane as a function of pressure and temperature. J. Solution Chem. **25**, 1163–1173 (1996)
40. Chernyak, Y.: Dielectric constant, dipole moment, and solubility parameters of some cyclic acid esters. J. Chem. Eng. Data **51**, 416–418 (2006)